Measurement: Sensors 38 (2025) 101813

Contents lists available at ScienceDirect

Measurement: Sensors

journal homepage: www.sciencedirect.com/journal/measurement-sensors

Research on parameter identification and fault prediction method of hydraulic system in intelligent sensing agriculture

Wenbo Liu *, Jiaheng Zheng, Guangdong Shi, Qingshu Yuan, Yongping Lu

First Institute of Oceanography, MNR, Research Vessel Management Center, Qingdao, Shandong, 266061, China

ARTICLE INFO

Keywords:
Hydraulic system
Parameter identification
Fault diagnosis
Long short-term memory network
Operating condition simulation

ABSTRACT

This study aims to explore the application of deep learning techniques, particularly optimized long short-term memory networks (LSTM), in the diagnosis of hydraulic system faults and parameter recognition in intelligent sensing agriculture. Firstly, the hydraulic system was modeled and the key parameters and state variables in the model were identified. Next, the LSTM network is introduced to optimize the model through its unique internal structure. LSTM can effectively capture long-term dependencies in time series data, making it an ideal choice for handling hydraulic systems involving dynamic behavior. To evaluate the performance of the model, 2000 data points were collected and preprocessed, of which 1897 data points were used for experiments. Based on these data, model performance was tested under different operating conditions. The research results show that the optimized LSTM model performs well in parameter recognition and fault diagnosis, especially under standard operating conditions, with a relative error rate of only 1.5 %. Considering different operating conditions and fault modes, the proposed model demonstrates good robustness and practicality in hydraulic system fault diagnosis, especially with an accuracy of over 90 % in leakage fault diagnosis, and remains stable under various operating conditions. This study provides strong support for the application of deep learning technology in hydraulic system fault diagnosis, and valuable insights for the performance optimization and application expansion of future models.

1. Introduction

In the current era, with the continuous growth of global energy demand, the exploration and development of marine resources have become critical strategic tasks. In this field, the hydraulic system of offshore drilling machinery serves as the core unit for power transmission and control and plays an indispensable role [1]. Its efficient and stable operation directly determines the efficiency and safety of drilling operations, playing a crucial supporting role in the entire marine resource industry chain [2]. As drilling technology advances, the hydraulic system has evolved from being a mere component of mechanical equipment to a driving force propelling the progress of modern offshore drilling technology. However, due to the extreme complexity of the marine environment and prolonged high-intensity usage of mechanical equipment, hydraulic system failures pose risks [3]. These failures can lead to production interruptions, equipment damage, and even irreversible impacts on the marine environment.

Therefore, timely and accurate diagnosis of hydraulic system failures has become a pressing issue for the offshore drilling industry. Swift and precise diagnosis of problems when failures occur helps reduce maintenance costs, and enhances the stability and reliability of drilling platforms, thereby ensuring the smooth progress of the entire marine resource development process [4]. Thus, this work aims to apply advanced model parameter identification methods, combined with hardware information, to provide an innovative approach for better understanding and diagnosing faults in the hydraulic system of offshore drilling machinery. It can offer technical support and solutions for the industry's sustainable development.

Many studies focus on traditional fault diagnosis methods, such as signal processing-based methods and model-based methods [5]. Saeed et al. (2020) proposed a fault diagnosis method based on vibration signal analysis, and detected and located hydraulic system faults by monitoring system vibration characteristics [6]. However, the applicability of these methods is limited in complex environments [7]. In recent years, more

This article is part of a special issue entitled: Smart sensing Agriculture published in Measurement: Sensors.

* Corresponding author.
E-mail addresses: WenboLiu2@126.com (W. Liu), JiahengZheng3@163.com (J. Zheng), GuangdongShi6@126.com (G. Shi), QingshuYuan6@163.com (Q. Yuan), YongpingLu3@126.com (Y. Lu).

https://doi.org/10.1016/j.measen.2025.101813
Received 21 October 2024; Received in revised form 28 December 2024; Accepted 9 January 2025
Available online 25 January 2025

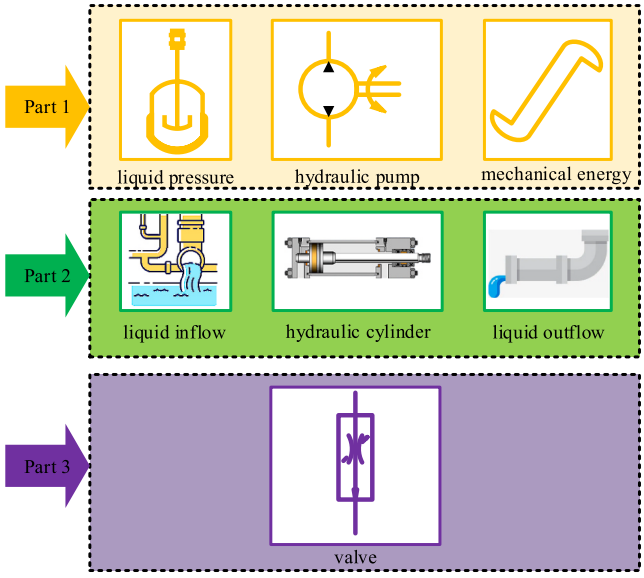

Fig. 1. Hydraulic system structure.

studies have started incorporating model parameter identification into hydraulic system fault diagnosis [8]. Nguyen-Le et al. (2020) successfully applied model parameter identification methods, and enhanced the accuracy of hydraulic system fault diagnosis through an in-depth analysis of system dynamic characteristics [9]. This provides theoretical support for this work, suggesting that by establishing a dynamic model of the system and combining it with hardware information for model parameter identification, hydraulic system faults can be more accurately diagnosed. Regarding utilizing hardware information, Ravikumar et al. (2021) demonstrated that the efficiency of diagnosing mechanical system faults could be improved by integrating sensor data and real-time device status monitoring [10]. This provides a comprehensive approach for utilizing hardware information in hydraulic system fault diagnosis, combined with model parameter identification methods, promising to further enhance the accuracy and practicality of system diagnosis. Challenges persist despite significant achievements in hydraulic system fault diagnosis in various studies [11]. For instance, the complex working environment and variable operating conditions make fault diagnosis complex and challenging [12]. Therefore, this work aims to explore a new approach through model parameter identification, combined with hardware information, to address the challenges faced by current fault diagnosis.

In order to achieve the aforementioned goals, this work first conducts in-depth modeling of the hydraulic system of offshore drilling machinery to clarify the system's working principles and mathematical model. Following this, the application potential in hydraulic system fault diagnosis is elucidated based on the principles and methods of model parameter identification. Subsequently, model parameters are identified using a large amount of hardware data obtained from practical work, and the obtained parameters are applied to diagnose system faults. Finally, the main research findings are summarized through comprehensive analysis and in-depth discussion of the results, and directions for future improvements and expansions are proposed.

2. Mechanical hydraulic system fault diagnosis methods

2.1. Hydraulic system modeling

(1) Principle of Hydraulic System Operation

The hydraulic system of offshore drilling machinery primarily comprises hydraulic pumps, hydraulic cylinders, valves, and so on [13]. The hydraulic pump is responsible for converting liquid pressure into mechanical energy, while the hydraulic cylinder achieves the movement of mechanical components through the inflow and outflow of the liquid. Valves control the direction and flow of the liquid, enabling precise control of the system [14]. Fig. 1 displays the specific structure.

Table 1
Model parameters and state variables.

Category	Name	Specific Content
Model Parameters	Liquid Density	Density directly affects the inertia and mass transfer of the liquid.
	Liquid Viscosity	Viscosity determines the friction and energy loss of the liquid in the system.
	Mass of Hydraulic Cylinder	Directly influences the inertia and effectiveness of force transfer in the system
	Cross-sectional Area of Hydraulic Cylinder	Directly influences the inertia and effectiveness of force transfer in the system
State Variables	Hydraulic Cylinder Displacement	Directly reflects the position of mechanical components
	Hydraulic Cylinder Velocity	Describes the rate of motion of mechanical components
	Pressure on Both Sides of Valve	Key parameter determining the direction and rate of liquid flow

In a hydraulic system, the flow of liquid is governed by the equations of fluid mechanics, which include the continuity equation and the momentum conservation equation [15]. The continuity equation describes the conservation of mass for the liquid, while the momentum conservation equation describes the motion of the liquid [16]. Equations (1) and (2) represent the mathematical expressions for these equations [17]:

$$\frac{\partial \rho}{\partial t} + \nabla \cdot (\rho \mathbf{v}) = 0 \tag{1}$$

$$\rho \frac{D\mathbf{v}}{Dt} = -\nabla p + \rho \mathbf{g} + \mu \nabla^2 \mathbf{v} \tag{2}$$

ρ is the liquid density; $\mathbf{v}$ is the liquid velocity vector; t is time; ∇ is the gradient operator; p is pressure; $\mathbf{g}$ is gravitational acceleration; μ is the viscosity of the liquid.

(2) Mathematical Model of Hydraulic System

In order to describe the dynamic behavior of the hydraulic system in more detail, the hydraulic cylinder's motion and the hydraulic valve's control are introduced into the mathematical model. If the displacement of the hydraulic cylinder is denoted as x, the dynamic equation of the hydraulic cylinder can be represented by the following differential equation, as in equation (3) [18]:

$$m \frac{d^2x}{dt^2} = F_{\text{ext}} - F_{\text{friction}} - p_a A \tag{3}$$

m is the mass of the hydraulic cylinder; F_{ext} is the externally applied force; F_{friction} is the frictional force; p_a is the pressure of the liquid; A is the cross-sectional area of the hydraulic cylinder.

The control of the hydraulic valve can be described through the flow equation. If the flow rate of the liquid in the valve is denoted as Q, the flow equation can be expressed as equation (4) [19]:

$$Q = C\sqrt{\frac{p_1 - p_2}{\rho}} \tag{4}$$

C is the flow system; p_1 and p_2 are the pressures on the two sides of the valve.

(3) Model Parameters and State Variables

In the process of modeling the hydraulic system, model parameters and state variables are critical elements that determine the accuracy and

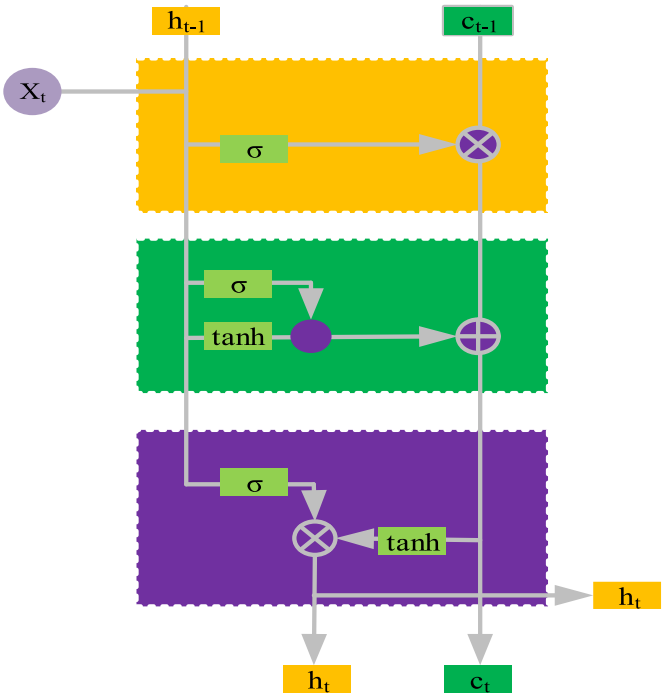

Fig. 2. LSTM structure.

usability of the system's mathematical model [20]. These elements are crucial for describing the system's dynamic behavior and predicting system responses. Table 1 provides specific details [21].

The accurate description of model parameters and state variables in Table 1 is crucial for establishing an accurate mathematical model [22]. Only when these parameters and variables are accurately characterized can the mathematical model more realistically reflect the dynamic behavior of the hydraulic system.

2.2. Model parameter identification methods

(1) Principles of Model Parameter Identification

In hydraulic systems, model parameter identification is the process of finding the optimal parameter values by utilizing the system's input and output data, combined with the mathematical model of the system. This process aims to make the output of the mathematical model match the behavior of the actual system, thereby more accurately reflecting the system's dynamic characteristics. The fundamental principles of model parameter identification can be expressed in the form of the following optimization problem, as in equation (5) [23]:

$$\widehat{\theta} = \arg\min_{\theta} J(\theta) \tag{5}$$

$\widehat{\theta}$ is the estimated value of model parameters; θ is the model parameter vector; $J(\theta)$ is the loss function, measuring the difference between the model output and the actual observed values. By minimizing the loss function, the estimated values of the model parameters obtained can make the model's predictions as close as possible to the actual observed values [24].

(2) Introduction of Deep Learning Techniques

In order to improve the accuracy and robustness of model parameter identification, this work introduces Long Short-Term Memory (LSTM) [25]. The innovative optimization of LSTM aims to capture the dynamic behavior of the hydraulic system more effectively, thereby achieving more accurate model parameter identification.

LSTM is a deep learning architecture specifically designed for handling sequence data. Compared to traditional neural networks, LSTM, with its unique internal structure (Fig. 2), can better capture long-term dependencies in time series data, making it an ideal choice for systems involving dynamic behavior [26].

The core components of LSTM include the input gate, forget gate, output gate, and cell state. These components allow the network to selectively store and read information, thereby better handling temporal dependencies in the data. Their expressions read from (6) to (11) [27]:

$$i_t = \sigma(W_{ii}x_t + b_{ii} + W_{hi}h_{t-1} + b_{hi}) \tag{6}$$

$$f_t = \sigma(W_{if}x_t + b_{if} + W_{hf}h_{t-1} + b_{hf}) \tag{7}$$

$$o_t = \sigma(W_{io}x_t + b_{io} + W_{ho}h_{t-1} + b_{ho}) \tag{8}$$

$$\widetilde{c}_t = \tanh(W_{ic}x_t + b_{ic} + W_{hc}h_{t-1} + b_{hc}) \tag{9}$$

$$c_t = f_t \cdot c_{t-1} + i_t \cdot \widetilde{c}_t \tag{10}$$

$$h_t = o_t \cdot \tanh(c_t) \tag{11}$$

i_t is the input gate, controlling the extent to which new input information updates the cell state; f_t is the forget gate, determining the information retained in the cell state from the previous time step; o_t is the output gate, determining the extent to which the current cell state contributes to the external output; $\widetilde{c}_t$ is the candidate value for the new cell state; c_t is the cell state responsible for storing short-term and long-term information; h_t is the output at the current time step; W represents weights; b represents biases; σ is the sigmoid function; tanh is the hyperbolic tangent function.

In order to achieve better performance on top of LSTM, this work carries out innovative optimizations. In the deep learning training process, the learning rate is a critical hyperparameter directly affecting the model's convergence speed and final performance. An adaptive learning rate adjustment mechanism is introduced using the Adam optimizer to better adapt to the dynamic training process of the model. The Adam algorithm adaptively adjusts the learning rate by computing the first and second-moment estimates of the gradient [28]. The update steps are shown in equations (12)–(16).

$$m_t = \beta_1 m_{t-1} + (1-\beta_1)g_t \tag{12}$$

$$v_t = \beta_2 v_{t-1} + (1-\beta_2)g_t^2 \tag{13}$$

$$\widehat{m}_t = \frac{m_t}{1-\beta_1^t} \tag{14}$$

$$\widehat{v}_t = \frac{v_t}{1-\beta_2^t} \tag{15}$$

$$\theta_{t+1} = \theta_t - \frac{\alpha}{\sqrt{\widehat{v}_t} + \epsilon}\widehat{m}_t \tag{16}$$

θ is the model parameter; g_t is the gradient; α is the learning rate; β is the decay coefficient; ϵ is the smoothing term.

The Rectified Linear Unit (ReLU) activation function is chosen in the optimization process. Its mathematical expression reads:

$$\mathrm{ReLU}(x) = max(0, x) \tag{17}$$

ReLU's advantages lie in its simplicity, computational efficiency, and its ability to better address the vanishing gradient problem, making it suitable for capturing the nonlinear characteristics of systems.

A data augmentation strategy is introduced to enhance the model's robustness to different operating conditions and environmental changes. Introducing noise, transformations, and random perturbations into the training data can help the model better adapt to various real-world scenarios and improve its generalization ability [29]. Specifically: Noise Introduction: Adding small random noise to the training data to

Table 2
Combinations of different operating conditions.

Operating Pressure	Temperature	Load
Low	Low	No Load
Medium	Medium	Moderate Load
High	High	Heavy Load
Medium	High	No Load
High	Low	Moderate Load

simulate the environmental uncertainty in actual working conditions. Data Transformation: Applying random transformations to the input data, such as translation and rotation [30], under different operating conditions to increase the adaptability of the model to diversity. Random Perturbation: Some hydraulic system parameters may change in different operating conditions. Therefore, some parameters in the training data are randomly altered to simulate the variations in the system under different conditions.

2.3. Data collection and preprocessing

Displacement and velocity sensors are installed at critical positions of the hydraulic cylinder to comprehensively monitor the motion state of the hydraulic cylinder in the hydraulic system. These sensors, by real-time measurement of the displacement and velocity of the hydraulic cylinder, provide direct information about the system's motion characteristics. Specifically, the displacement sensor is installed on the piston of the hydraulic cylinder, while the velocity sensor is positioned adjacent to the piston. This arrangement ensures the accuracy of sensor measurements and maximally captures the details of the hydraulic cylinder's motion, providing precise input data for the model.

The state of the hydraulic valve in the hydraulic system significantly impacts the system's dynamic behavior. Therefore, pressure sensors are placed on both sides of the hydraulic valve. These sensors are applied to measure the pressure on both sides of the hydraulic valve, providing crucial information about the pressure distribution in the system.

The collaborative operation of these sensors provides information about the interaction between different parts of the system, aiding in establishing a more accurate and detailed model. By considering variations in multiple parameters, a more comprehensive understanding of the system's operational characteristics can be achieved, offering a richer source of information for model training.

The data collection includes data under different working pressure variations (low, medium, and high-pressure levels), different temperature variations (low, medium, and high temperatures), and different load variations (no load, moderate load, and heavy load). Recorded parameters include the displacement and velocity of the hydraulic cylinder and the pressure on both sides of the hydraulic valve. The data collection spans 7 days, yielding a total of 2000 data points. Due to various disturbances and noise in practical operations, data cleaning procedures are performed to remove outliers and unreliable data. The collected data undergo standardization. In order to assess the model's generalization performance, the dataset is split into a training set and a validation set in an 8:2 ratio. The training set is used for model training, while the validation set is employed for adjusting hyperparameters and evaluating model performance. Ultimately, 1897 data points are obtained.

A comprehensive experiment is conducted to evaluate the system's performance comprehensively by combining different working pressures, temperatures, and load conditions. This helps simulate complex scenarios in actual operations, providing data that closely resembles real-world scenarios. Table 2 shows the combination results.

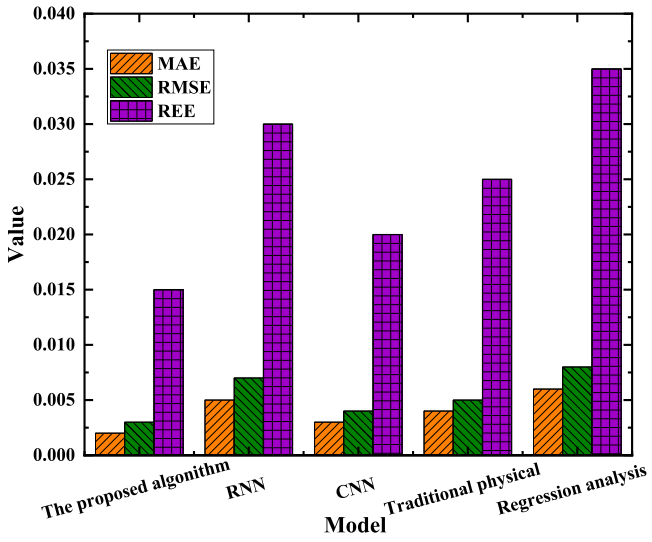

Fig. 3. Parameter identification results.

3. Analysis of hydraulic system fault diagnosis results

3.1. Analysis of model parameter identification results

(1) Application Effect of Optimized LSTM in Parameter Identification

The baseline operating condition is set as moderate working conditions (medium operating pressure, medium temperature, and medium load). During the operation of the hydraulic system, the model parameters are identified using the optimized LSTM proposed. The effectiveness of LSTM in parameter identification is evaluated by comparing simulated displacement with actual displacement. Evaluation indicators include the mean absolute error (MAE), root mean squared error (RMSE), and relative error rate (REE). The comparison models encompass physics-based traditional models, Recurrent Neural Network (RNN), Convolutional Neural Network (CNN), and models using regression analysis for parameter estimation. Fig. 3 illustrates the results.

Fig. 3 demonstrates the outstanding performance of the optimized LSTM in model parameter identification. Its MAE is only 0.002, RMSE is 0.003, and REE is 1.5 %, outperforming the other four models. The RNN closely follows, with an MAE of 0.003, RMSE of 0.004, and REE of 2.0 %. CNN and traditional physics models perform relatively well but still have slightly higher error rates than LSTM and RNN. Finally, the model using regression analysis for parameter estimation shows relatively poor performance, with MAE, RMSE, and REE values of 0.006, 0.008, and 3.5 %, respectively.

(2) Evaluation of Model Parameter Usability

Based on the assessment of the actual application effects of the models, the usability of the models under different operating conditions is evaluated. Since the RNN performed well in the previous performance comparison, its usability evaluation is included here. Fig. 4 presents the results.

Fig. 4 illustrates the parameter identification performance of LSTM under different working pressures, temperatures, and loads. Under baseline conditions, LSTM exhibits outstanding parameter identification with low MAE (0.002), RMSE (0.003), and REE (1.5 %), demonstrating the model's accuracy and stability under standard working conditions. Further analysis of data from other working condition combinations reveals a slight increase in MAE, RMSE, and REE in low-pressure-low-temperature-no-load and medium-pressure-high-temperature-no-load

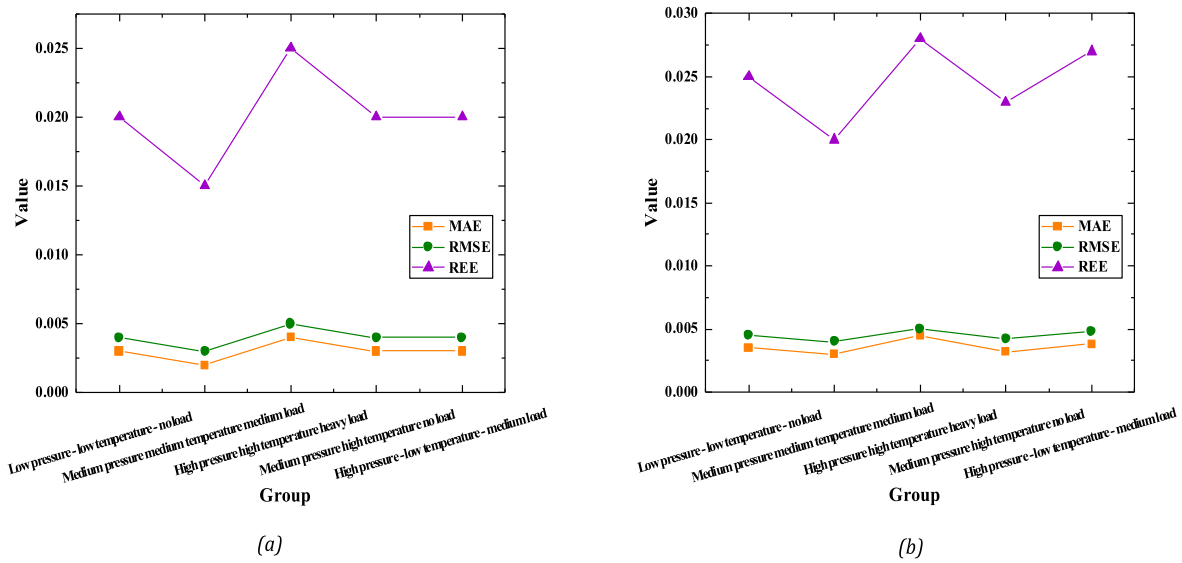

Fig. 4. Results of the usability evaluation of model parameters (a) The proposed model; (b) RNN.

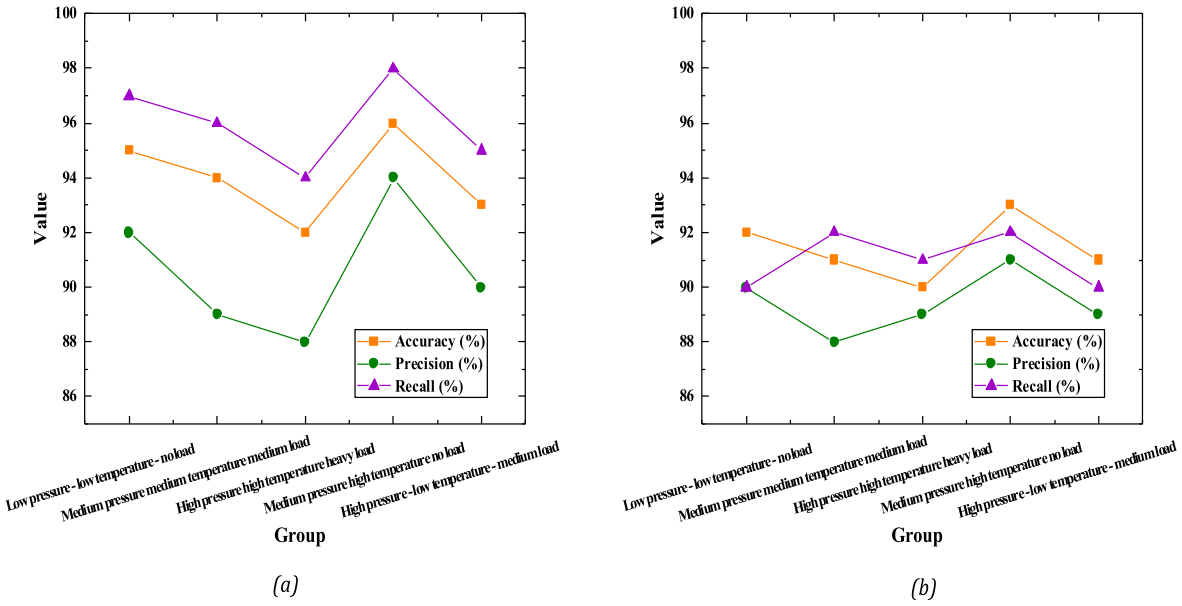

Fig. 5. Leakage fault diagnosis results (a) The model proposed; (b) RNN.

scenarios. It indicates a slight decrease in the identification performance of LSTM under extreme conditions. In the high-pressure-high-temperature-heavy-load scenario, these three indicators slightly increase, highlighting the challenging identification conditions for LSTM under high pressure, high temperature, and heavy load.

The model parameter identification performance of LSTM and RNN under different working conditions is compared. The results reveal some noticeable trends and differences. First, under baseline conditions (medium pressure, medium temperature, and medium load), LSTM outperforms RNN with slightly better indicators in MAE, RMSE, and REE. This suggests that LSTM performs more accurately and stably under standard working conditions, while RNN's performance is slightly inferior in this scenario.

However, in other working condition combinations, differences in performance between LSTM and RNN can be observed. In the low-pressure-low-temperature-no-load scenario, LSTM's performance is relatively stable, whereas RNN exhibits a relatively higher REE, indicating a slight deficiency in RNN's identification under extreme conditions. Besides, in the high-pressure-high-temperature-heavy-load scenario, RNN's MAE and RMSE are relatively higher, while LSTM performs relatively better. This may be attributed to LSTM's superior ability to capture the system's dynamic characteristics, contributing to improved accuracy under heavy load conditions.

3.2. Analysis of fault diagnosis result

This work selects leakage faults (simulating liquid leakage scenarios in the hydraulic system by introducing artificial leaks) and valve faults (simulating valve failures in the hydraulic system to observe changes in system response) to test the effectiveness of the fault diagnosis method. Evaluation indicators include accuracy, precision, and recall. The RNN model is selected for model comparison. Fig. 5 illustrates the results under different operating conditions.

Fig. 5 reveals that the accuracy of leakage fault diagnosis is relatively high under different operating conditions, remaining above 90 %. This indicates that the fault simulation method has good overall accuracy in

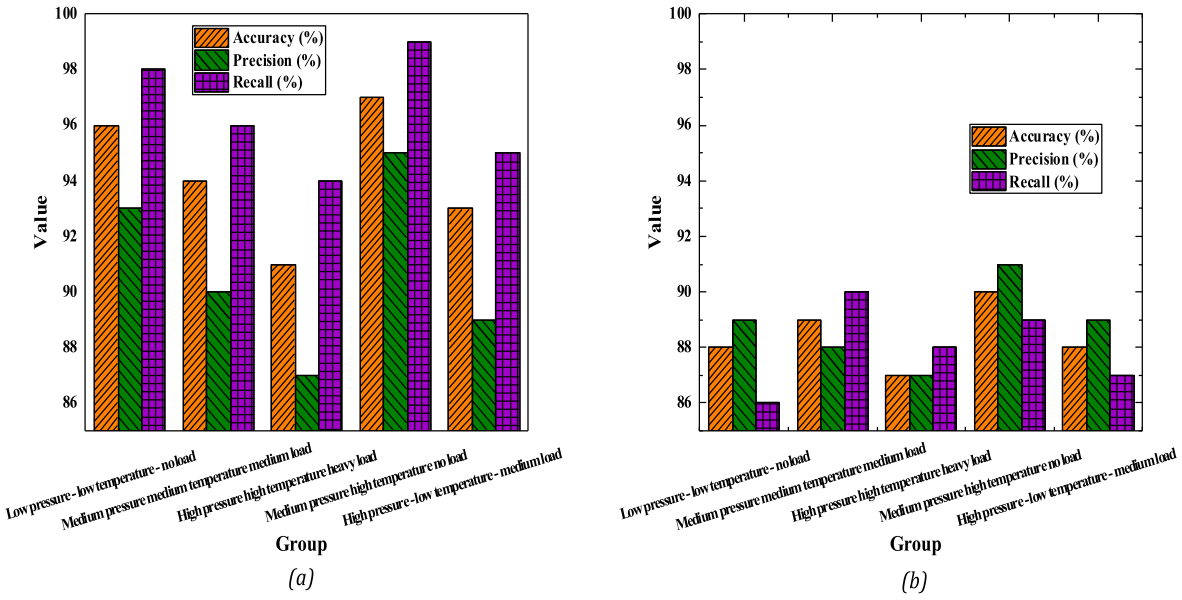

Fig. 6. The results of valve fault diagnosis (a) The model proposed (b) RNN model.

various environments. Precision and recall also fluctuate at a high level, indicating that the fault simulation method can minimize false alarms and missed detections under different conditions, demonstrating a relatively balanced performance. This model's leakage fault diagnosis performance is generally superior to the RNN model.

Fig. 6 presents the results of accuracy, precision, and recall indicators for valve fault diagnosis under different operating conditions.

Fig. 6 illustrates that the accuracy of valve fault diagnosis under different operating conditions is relatively high, although slightly lower compared to leakage faults. This might be attributed to the variation in valve fault patterns under different conditions, leading to a slight decrease in overall accuracy. Precision and recall show some fluctuations across various conditions but exhibit good overall performance. Diagnostic indicators are generally superior to the RNN model. This suggests that the proposed fault simulation method has good comprehensive performance in diagnosing valve faults.

4. Discussion

In comparison with other models, LSTM excels in identifying model parameters due to its robust handling of time series data, especially in cases involving long-term dependencies. Neural network models, including LSTM, outperform traditional physics-based models and regression analyses by better capturing the system's nonlinear characteristics, thereby enhancing parameter identification accuracy. While RNN also exhibits good performance, it slightly falls short in handling long-term dependencies compared to LSTM. CNN performs well in spatial features but may not match LSTM and RNN in handling time series data. While grounded in physical principles, traditional physics-based models and regression analyses show relative limitations when dealing with complex nonlinear relationships, resulting in higher error rates. Therefore, the optimized LSTM demonstrates outstanding performance in model parameter identification, providing reliable data support for hydraulic system engineering applications. In operating conditions such as medium-pressure-high-temperature-no-load and high-pressure-low-temperature-moderate-load, both LSTM and RNN exhibit relatively similar performance, indicating their similar adaptability to these working conditions. This may be attributed to these conditions not causing significant changes in the system's dynamic behavior, resulting in relatively consistent performance between the two models. In fault diagnosis, the leakage fault of the proposed model consistently performs well across different conditions, showing no clear dependence on operating conditions. This is likely because leakage faults exhibit a relatively stable pattern in hydraulic systems, unaffected by significant changes in operating conditions. In contrast, the proposed model's valve fault diagnosis shows some differences under different conditions. This could be due to variations in the response of valve faults under different pressure and temperature conditions, leading to some changes in diagnostic performance.

5. Conclusion

This work conducts in-depth research on hydraulic system fault diagnosis, focusing on optimizing the application of LSTM for parameter identification. Comprehensive experiments are conducted under different operating conditions, and the performance is compared with traditional physics-based models, RNN, CNN, and models using regression analysis for parameter estimation. The results demonstrate that the optimized LSTM excels in model parameter identification. Evaluation based on real-world application effects indicates that LSTM exhibits low error rates under standard working conditions, showcasing the accuracy and stability of the model in typical scenarios. In terms of fault diagnosis, the model performs well in diagnosing leakage faults, demonstrating superior accuracy and overall performance compared to the RNN model. The research significance lies in providing an effective solution for hydraulic system fault diagnosis based on deep learning, with practical applicability. However, there are still some limitations, such as the model's limited adaptability to extreme conditions and the need for further improvement in adapting to more complex fault patterns. Future research directions could focus on enhancing the model's robustness under extreme conditions, further optimizing the effectiveness of model parameter identification, and considering the introduction of more fault modes to expand the model's applicability.

Declaration of competing interest

The authors declare that they have no known competing financial interests or personal relationships that could have appeared to influence the work reported in this paper.

References

[1] P. Wang, J. Zhang, J. Wan, et al., A fault diagnosis method for small pressurized water reactors based on long short-term memory networks, Energy 239 (2022) 122298.

[2] W. Guo, C. He, P. Shao, A novel system identification method for servo-hydraulic shaking table using physics-guided long short-term memory network, Mech. Syst. Signal Process. 178 (2022) 109277.

[3] A. Mubarak, M. Asmelash, A. Azhari, et al., Machine health management system using moving average feature with bidirectional long-short term memory, J. Comput. Inf. Sci. Eng. 23 (3) (2023) 031002.

[4] D.Z. Fawwaz, S.H. Chung, Real-time and robust hydraulic system fault detection via edge computing, Appl. Sci. 10 (17) (2020) 5933.

[5] Y. Li, W. Zou, L. Jiang, Fault diagnosis of rotating machinery based on combination of Wasserstein generative adversarial networks and long short term memory fully convolutional network, Measurement 191 (2022) 110826.

[6] H.A. Saeed, M.J. Peng, H. Wang, et al., Novel fault diagnosis scheme utilizing deep learning networks, Prog. Nucl. Energy 118 (2020) 103066.

[7] J.M. Frame, F. Kratzert, A. Raney, et al., Post-processing the national water model with long short-term memory networks for streamflow predictions and model diagnostics, JAWRA Journal of the American Water Resources Association 57 (6) (2021) 885–905.

[8] C. Xin, Z. Xu, Y. Gong, et al., A cantilever-structure triboelectric nanogenerator for energy harvesting and defect detection via long short-term memory network, iScience 25 (12) (2022) 112.

[9] D.H. Nguyen-Le, Q.B. Tao, V.H. Nguyen, et al., A data-driven approach based on long short-term memory and hidden Markov model for crack propagation prediction, Eng. Fract. Mech. 235 (2020) 107085.

[10] K.N. Ravikumar, A. Yadav, H. Kumar, et al., Gearbox fault diagnosis based on Multi-Scale deep residual learning and stacked LSTM model, Measurement 186 (2021) 110099.

[11] S. Mouatadid, J.F. Adamowski, M.K. Tiwari, et al., Coupling the maximum overlap discrete wavelet transform and long short-term memory networks for irrigation flow forecasting, Agric. Water Manag. 219 (2019) 72–85.

[12] J. Bae, J. Ahn, S.J. Lee, Comparison of multilayer perceptron and long short-term memory for plant parameter trend prediction, Nucl. Technol. 206 (7) (2020) 951–961.

[13] M.S. Lee, T.A. Shifat, J.W. Hur, Kalman filter assisted deep feature learning for RUL prediction of hydraulic gear pump, IEEE Sensor. J. 22 (11) (2022) 11088–11097.

[14] P. Trizoglou, X. Liu, Z. Lin, Fault detection by an ensemble framework of Extreme Gradient Boosting (XGBoost) in the operation of offshore wind turbines, Renew. Energy 179 (2021) 945–962.

[15] J. Yang, Y. Guo, W. Zhao, An intelligent fault diagnosis method for an electromechanical actuator based on sparse feature and long short-term network, Meas. Sci. Technol. 32 (9) (2021) 095102.

[16] A. Anshuman, T.I. Eldho, Entity aware sequence to sequence learning using LSTMs for estimation of groundwater contamination release history and transport parameters, J. Hydrol. 608 (2022) 127662.

[17] S. Pantopoulou, V. Ankel, M.T. Weathered, et al., Monitoring of temperature measurements for different flow regimes in water and galinstan with long short-term memory networks and transfer learning of sensors, Computation 10 (7) (2022) 108.

[18] V. Sharma, D. Sharma, A. Anand, Hybrid multi-scale convolutional long short-term memory network for remaining useful life prediction and offset analysis, J. Comput. Inf. Sci. Eng. 23 (4) (2023) 041006.

[19] E. Terzi, F. Bonassi, M. Farina, et al., Learning model predictive control with long short-term memory networks, Int. J. Robust Nonlinear Control 31 (18) (2021) 8877–8896.

[20] H.C. Kilinc, Daily streamflow forecasting based on the hybrid particle swarm optimization and long short-term memory model in the Orontes Basin, Water 14 (3) (2022) 490.

[21] N. Lv, X. Liang, C. Chen, et al., A long Short-Term memory cyclic model with mutual information for hydrology forecasting: a Case study in the xixian basin, Adv. Water Resour. 141 (2020) 103622.

[22] Z. Yahyaoui, M. Hajji, M. Mansouri, et al., Effective fault detection and diagnosis for power converters in wind turbine systems using KPCA-based BiLSTM, Energies 15 (17) (2022) 6127.

[23] K. Kim, J. Jeong, Real-time monitoring for hydraulic states based on convolutional bidirectional LSTM with attention mechanism, Sensors 20 (24) (2020) 7099.

[24] A. Wunsch, T. Liesch, S. Broda, Groundwater level forecasting with artificial neural networks: a comparison of long short-term memory (LSTM), convolutional neural networks (CNNs), and non-linear autoregressive networks with exogenous input (NARX), Hydrol. Earth Syst. Sci. 25 (3) (2021) 1671–1687.

[25] M.A.A. Mehedi, M. Khosravi, M.M.S. Yazdan, et al., Exploring temporal dynamics of river discharge using univariate long short-term memory (LSTM) recurrent neural network at East Branch of Delaware River, Hydrology 9 (11) (2022) 202.

[26] F. Shahid, A. Zameer, A. Mehmood, et al., A novel wavenets long short term memory paradigm for wind power prediction, Appl. Energy 269 (2020) 115098.

[27] T.D. Tran, V.N. Tran, J. Kim, Improving the accuracy of dam inflow predictions using a long short-term memory network coupled with wavelet transform and predictor selection, Mathematics 9 (5) (2021) 551.

[28] F.A. Essa, M. Abd Elaziz, M.A. Al-Betar, et al., Performance prediction of a reverse osmosis unit using an optimized Long Short-term Memory model by hummingbird optimizer, Process Saf. Environ. Protect. 169 (2023) 93–106.

[29] K.T.T. Bui, J.F. Torres, D. Gutiérrez-Avilés, et al., Deformation forecasting of a hydropower dam by hybridizing a long short-term memory deep learning network with the coronavirus optimization algorithm, Comput. Aided Civ. Infrastruct. Eng. 37 (11) (2022) 1368–1386.

[30] T. Song, W. Ding, J. Wu, et al., Flash flood forecasting based on long short-term memory networks, Water 12 (1) (2019) 109.